Colloid Polym Sci (2005) 283: 1123–1130
DOI 10.1007/s00396-004-1258-1

Tomohisa Yamaguchi
Keisuke Kimura
Akira Tsuchida
Tsuneo Okubo
Mitsuhiro Matsumoto

Drying dissipative structures of the aqueous suspensions of monodisperse bentonite particles

Received: 27 September 2004
Accepted: 5 November 2004
Published online: 19 January 2005

T. Yamaguchi · K. Kimura · A. Tsuchida
Department of Applied Chemistry,
Gifu University, Gifu, 501-1193, Japan

T. Okubo (✉)
Institute for Colloidal Organization,
Hatoyama 3-1-112, Uji, Kyoto
611-0012, Japan
E-mail: okubotsu@ybb.ne.jp
Fax: +81-774-328270

M. Matsumoto
Department of Chemistry, Faculty of Arts and Sciences, Tokushima University,
Tokushima, 770-8502, Japan

Abstract Macroscopic and microscopic dissipative structural patterns formed in the course of drying the fractionated and monodisperse bentonite particles (plate-like in their shape) in aqueous deionized suspension and in the presence of NaCl have been studied on a cover glass. The patterns coexisted with the broad ring of the hill accumulated with the particles and with the round hills are formed around the outside edges of the film and in the center, respectively, in the macroscopic scale. By the addition of NaCl the pattern shifts from the broad ring to the round hill in the center. The spoke-like cracks, which have been observed for the suspensions of the spherical particles so often hitherto, are not observed at all for the bentonite suspensions. The characteristic convection flow of the particles and the interactions among the particles and substrate are important for the macroscopic pattern formation. Wrinkled, branch-like and/or star-like fractal patterns are observed in the microscopic scale. These patterns are determined mainly by the electrostatic and polar interactions between the particles and/or between the particle and the substrate in the course of drying.

Keywords Drying dissipative structure · Pattern formation · Bentonite · Broad ring pattern · Fractal pattern

Introduction

Generally speaking, most structural patterns in nature and experiments in the laboratory form via self-organization accompanied with the dissipation of free energy and in the non-equilibrium state. Among several factors in the free energy dissipation, evaporation at the liquid surface and convection induced by the earth's gravity are very important.

In previous papers from our laboratory [1, 2], drying dissipative patterns on a cover glass have been studied for colloidal crystal suspensions of colloidal silica and polystyrene spheres. Quite similar macroscopic and microscopic structural patterns formed between the two kinds of spheres. The broad ring patterns of the hill accumulated with spheres in the outside edges and the spoke-like and ring-like cracks formed in the macroscopic scale. The existence of the small circle convection cells proposed by Terada [3–5] was supported. Structural patterns were observed in the course of drying the suspension of Chinese black ink on a cover glass and in a dish [6]. The clear broad ring and spoke-like patterns of the rims accumulated with particles formed especially in the central region of the film. Interestingly, the primitive vague patterns of valleys were formed already in the concentrated suspensions before dryness and they grow toward fine cracks in the course of solidification. Branch-like fractal patterns of the sphere association were observed in the microscopic scale. Capillary forces between the neighboring spheres at the air–liquid inter-

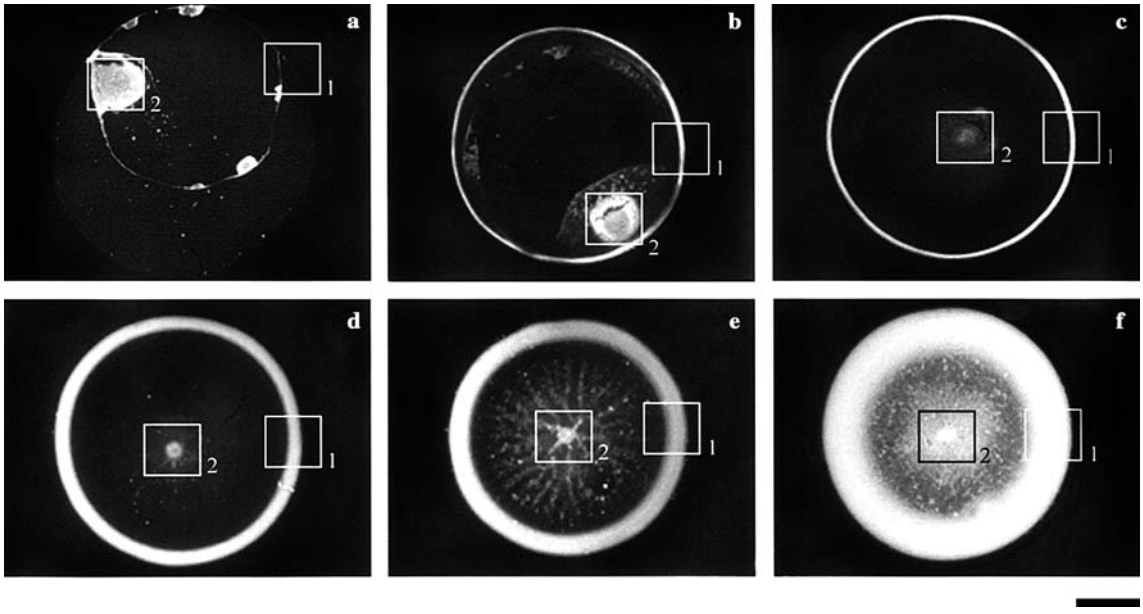

Fig. 1 Patterns formed for 2p7f particles at 25°C. **a** $w = 4.6\times10^{-4}$ mg/mL, **b** 0.046 mg/mL, **c** 0.092 mg/mL, **d** 0.46 mg/mL, **e** 0.92 mg/mL, **f** 4.6 mg/mL. In water, 0.05 mL, length of the bar is 2.0 mm. Extended pictures of the area given by squares are shown in Figs. 2, 3, 4 and 5

face and the different rates of convection flows of water and spheres at the drying front were important for the pattern formation. Quite recently, drying dissipative structures of a series of colloidal silica spheres ranging from 29 nm to 1 μm in diameter were studied in the aqueous deionized suspension [7].

The drying structures have been studied further for the linear-type macrocations, i.e., poly(allylamine hydrochloride) [8]. Macroscopic broad ring patterns formed. Furthermore, beautiful string-like fractal patterns were observed in the microscopic scale. The drying experiments were made for *n*-dodecyltrimethylammonium chloride [9]. Recently, a series of anionic detergent molecules, sodium *n*-alkyl sulfates (*n*-alkyl = *n*-hexyl, *n*-octyl, *n*-decyl, *n*-dodecyl, *n*-hexadecyl and *n*-octadecyl) were used for study of the drying dissipative patterns [10]. Broad ring patterns formed in the macroscopic scale. Star-like, branch-like, arc-like and small block-like microstructures were also observed. The convection of water and detergents at different rates under gravity and the translational and rotational Brownian movement of the latter were important for the macroscopic pattern formation. Microscopic patterns were also determined by the translational Brownian diffusion of the detergent molecules and the electrostatic and the hydrophobic interactions between detergents and/or between the detergents and substrate in the course of the solidification.

From these studies on drying structures, very similar macroscopic broad ring patterns formed irrespective of kind of solutes and their concentrations. Microscopic patterns such as branch-like, string-like, arc-like and small block-like ones were, however, reflected in the shape, size and flexibility of the solute molecules. In this work, monodisperse bentonite particles, which are obtained by the repeated centrifugation technique and highly monodisperse in their size, are studied in detail. The main purpose of this work is, of course, to study the shape effect between the anisotropic-shaped and spherical particles in the drying dissipative patterns.

Experimental

Materials

Monodisperse bentonite particles were obtained by the fractional repeated centrifugation technique. The details of the sample preparation were described in the previous papers [11, 12]. Quite recently several researchers applied the centrifugation technique to obtain the monodisperse particles of bentonite [13, 14]. Diagonal diameter of the particles, code 2p7f was 324 nm from the electron microscopy. These colloidal samples were deionized with a mixed bed of cation- and anion-exchange resins more than 2 years. It takes a long time before complete deionization is achieved, since the deionization proceeds between the two solid–liquid phases one after another, i.e., between colloidal particles and water and then water and the resins. Furthermore, bentonites are swelled and very porous in their surfaces. The deionized suspension thus obtained was blue and transparent, which supports clearly formation of the liquid-like distribution of the particles by the extended electrical double-layers. It should be mentioned here that the

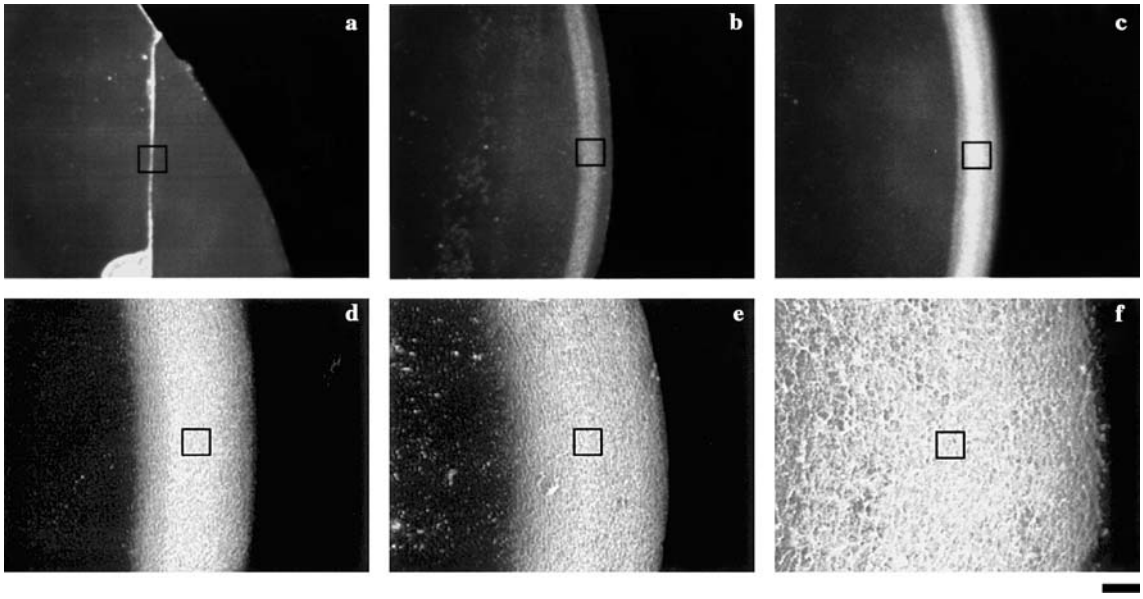

Fig. 2 Patterns formed for 2p7f particles at 25°C. Series 1, **a** $w = 4.6\times10^{-4}$ mg/mL, **b** 0.046 mg/mL, **c** 0.092 mg/mL, **d** 0.46 mg/mL, **e** 0.92 mg/mL, **f** 4.6 mg/mL. In water, 0.05 mL, length of the bar is 200 μm

crystal-like distribution of the particles was not formed since the single crystals were not observed for the suspension. The water used for the sample purification and preparation was purified by a Milli-Q reagent grade system (Milli-RO5 plus and Milli-Q plus, Millipore, Bedford, MA, USA).

Observation of the dissipative structures

An amount of 0.05 mL of the aqueous suspension of the bentonite particles was dropped carefully and gently on a micro cover glass (30 mm×30 mm, thickness No.1, 0.12 to 0.17 mm, Matsunami Glass Co., Kishiwada, Osaka) in a dish (60 mm in diameter, 15 mm in depth, Petri Co., Tokyo). The cover glass was used without further rinsing in this work. The extrapolated value of the contact angle for pure water was $31 \pm 0.2°$ from the drop profile of a small amount of water (0.2, 0.4, 0.6 and

Fig. 3 Patterns formed for 2p7f particles at 25°C. Series 1, **a** $w = 4.6\times10^{-4}$ mg/mL, **b** 0.046 mg/mL, **c** 0.092 mg/mL, **d** 0.46 mg/mL, **e** 0.92 mg/mL, **f** 4.6 mg/mL. In water, 0.05 mL, length of the bar is 2 μm

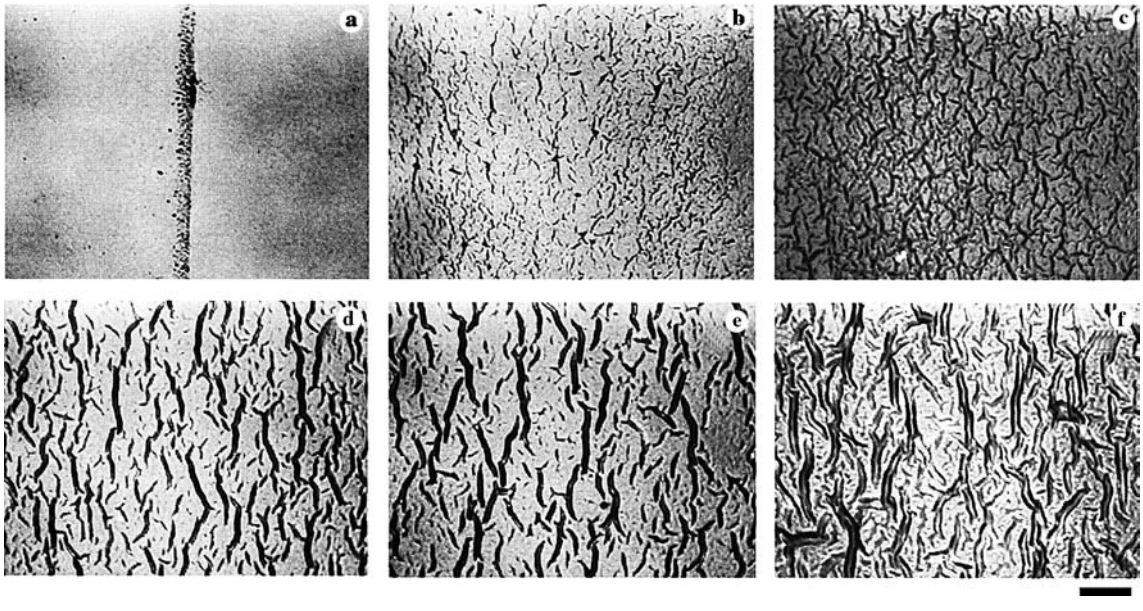

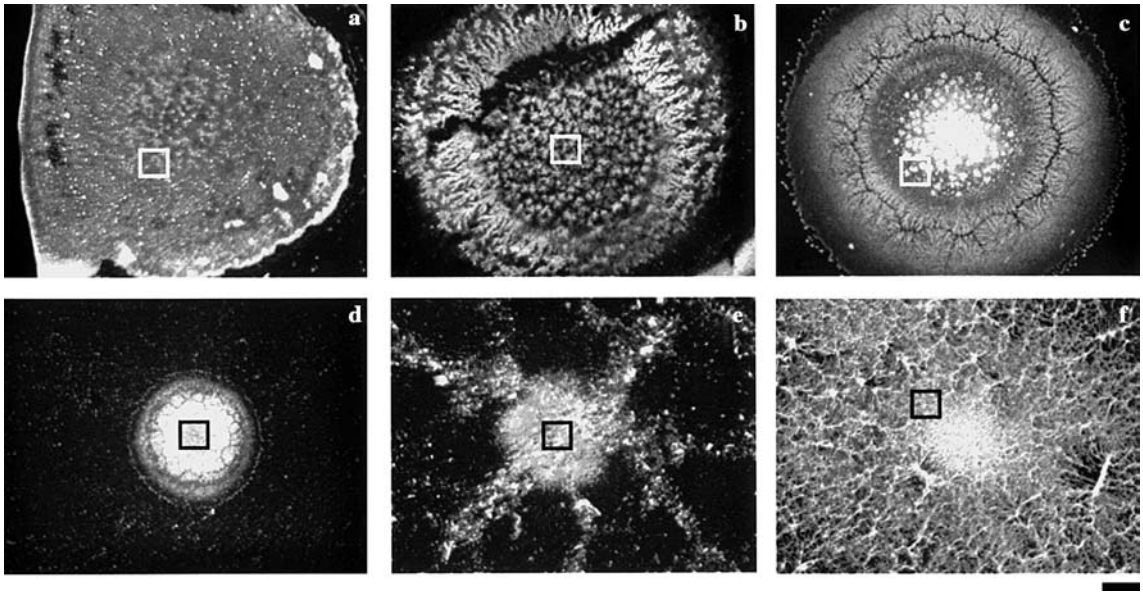

Fig. 4 Patterns formed for 2p7f particles at 25°C. Series 2, **a** $w = 4.6\times10^{-4}$ mg/mL, **b** 0.046 mg/mL, **c** 0.092 mg/mL, **d** 0.46 mg/mL, **e** 0.92 mg/mL, **f** 4.6 mg/mL. In water, 0.05 mL, length of the bar is 200 μm

0.8 μL) on the cover glass. A pipet (1 mL, disposable serological pipet, Corning Lab. Sci. Co.) was used for the dropping. Observation of the macroscopic and microscopic drying patterns was made for the film formed after the suspension was dried up completely on a cover glass in a room air-conditioned at 25 °C and 65% in humidity of the air. Concentrations of the particles ranged from 4.6×10^{-4} mg/mL to 4.6 mg/mL.

Macroscopic dissipative structures were observed with a digital HD microscope (type VH-7000, Keyence Co., Osaka) and a Canon EOS 10 camera with macro-lens (EF 50 mm, $f = 2.5$) and a life-size converter EF. Microscopic structures were observed with a laser 3D profile microscope (type VK-8500, Keyence) and a metallurgical microscope (Axiovert 25CA, Carl-Zeiss, Jena GmbH).

Fig. 5 Patterns formed for 2p7f particles at 25°C. Series 2, **a** $w = 4.6\times10^{-4}$ mg/mL, **b** 0.046 mg/mL, **c** 0.092 mg/mL, **d** 0.46 mg/mL, **e** 0.92 mg/mL, **f** 4.6 mg/mL. In water, 0.05 mL, length of the bar is 2 μm

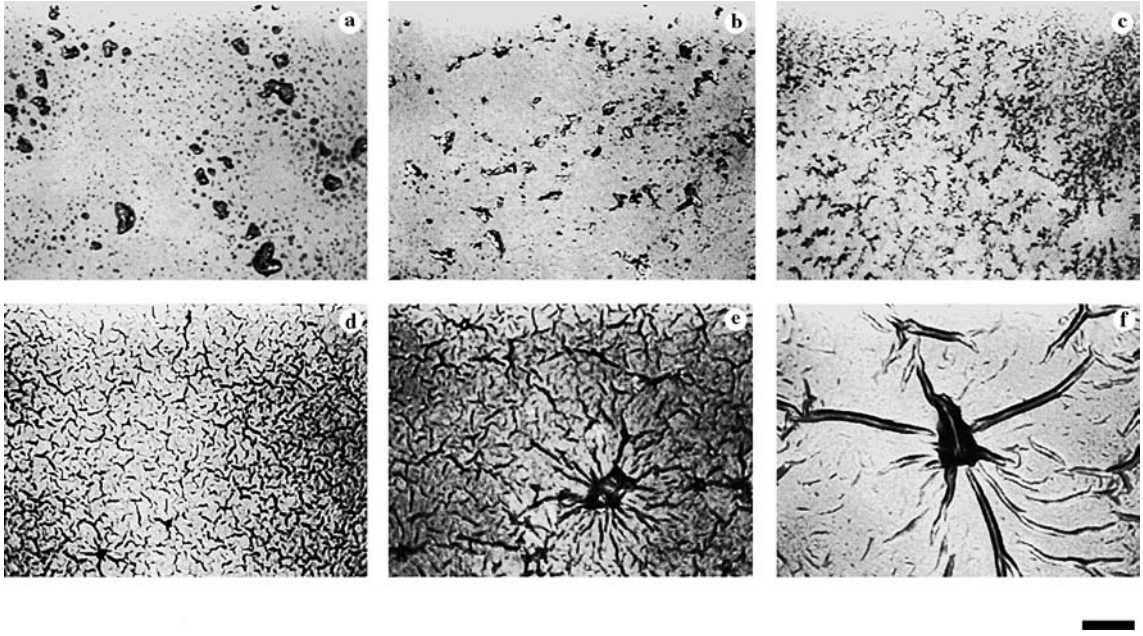

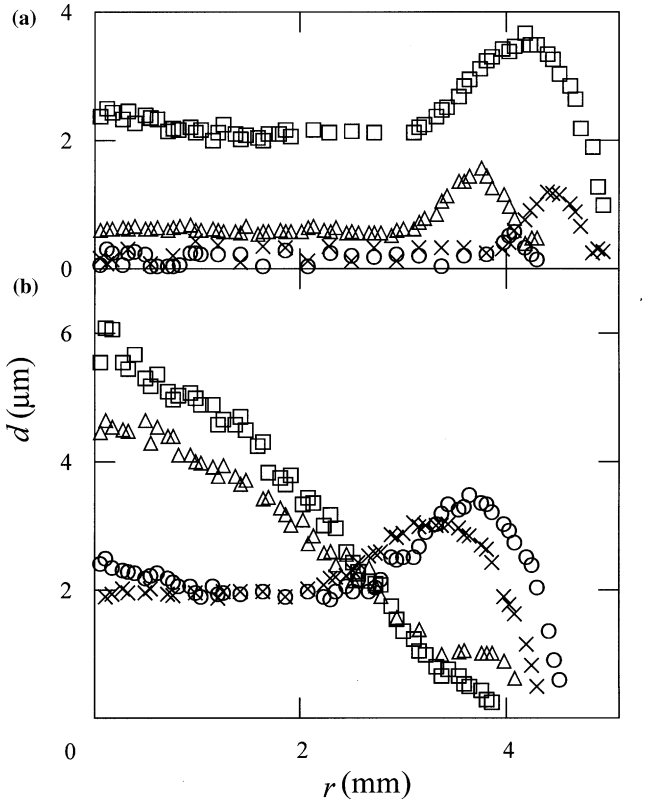

Fig. 6 Thickness (d) of the dried film as a function of radius (r) at 25°C. In water, 0.05 mL, **a** deionized suspensions, *open circle* $w = 0.092$ mg/mL, *X* 0.46 mg/mL, *open triangle* 0.92 mg/mL, *open square* 4.6 mg/mL; **b** with NaCl, $w = 4.6$ mg/mL, *open circle* NaCl = 0 M, *X* 1×10^{-5} M, *open triangle* 1×10^{-4} M, *open square* 1×10^{-3} M

Results and discussion

Particle concentration dependency

Figure 1 shows the typical patterns formed in the drying the suspensions of 2p7f particles at the concentrations ranging from 4.6×10^{-4} mg/mL to 4.6 mg/mL. The broad ring patterns were observed and their widths increased sharply as particle concentration increased. A main cause for the broad ring formation is due to the convection flow of water and the colloidal particles in the different rates, where the rate of the latter will be slower than that of the former under gravity. Especially, flow of the particles from the center area toward the outside edges in the lower layer of the liquid drop, which was observed on a digital HD microscope directly from the movement of the very rarely occurred aggregates of the particles, is important [6]. The convection flow is enhanced by the evaporation of water at the liquid surface, resulting lowering of the suspension temperature in the upper region. When the particles reach the edges of the drying frontier at the outside region of the liquid, a part of the particles will turn to upward and go back to the center region. However, movement of the most particles may stop at the frontier region by the disappearance of water. This process must be followed by the broad ring accumulation of the particles near the round edges. It should be noted that the broad ring formation has been observed for all the solutions and suspensions examined by our group [1, 2, 6–10, 15–18] and further by other researchers [19–21]. Recently, microgravity experiments were made for the observation of the drying dissipative patterns of deionized suspension of colloidal silica spheres [22]. Surprisingly, the broad ring patterns did not disappear even in microgravity. This supports that both the gravitational and the Marangoni convections contribute for the broad ring formation on earth but the latter is still important in microgravity.

We should note here that there appeared a hill in the center region in addition of the broad ring especially at the high particle concentrations. These hills in the central area have not been observed for the suspensions of any kind of spherical particles hitherto. The rotational movement must be highly restricted for the anisotropic-shaped particles like plate-like ones in this work, and the sliding movement will be in major especially in the area close to the substrate plane. This restricted Brownian movement must be correlated deeply to the appearance of the hill in the center. However, mechanism of the coexistence of the two patterns is not so clear yet, because the visualized observation of the convection cells was not easy experimentally.

Figure 2 shows the extended patterns of the broad ring parts shown by the squares of a series 1 in Fig. 1. The length of the bar is 200 μm. The surfaces of the broad rings formed in the outside regions look very rough, which may support the random accumulation of the plate-like particles. However, much more extended microscopic patterns of the broad ring parts shown in Fig. 3 demonstrate clearly that the particles are stacked rather regularly forming the short hills oriented circularly. It should be noted here that the black area is not cracks but hills. Here, the length of the bar in Fig.3 is 2 μm.

Figure 4 shows the extended patterns of the central area shown by the squares of a series 2 in Fig. 1. The length of the bar is 200 μm. Very beautiful fractal patterns of the particle accumulation are observed. Much more extended patterns are shown in Fig. 5 for the square area of Fig. 4. Clearly, short and long hills distribute radially and in the fractal features. Here again black parts are higher than the white regions in Fig. 5. It should be mentioned here that no spoke-like and circle cracks were not observed for 2p7f particles at all.

Figure 6a shows the thickness of the film as a function of the distance from the center (r) in the deionized suspension. The experiments were made directly using a laser 3D profile microscope. Surprisingly, the d–r pro-

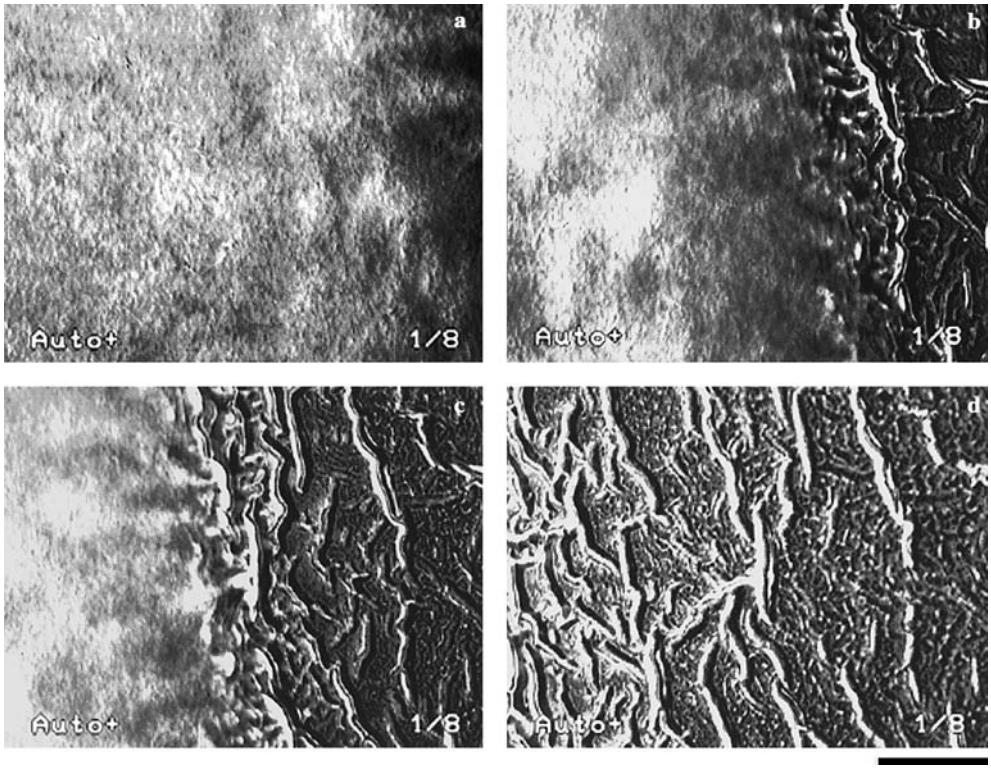

Fig. 7 Patterns formed for 2p7f particles at 25°C. In water, 0.05 mL, $w = 4.6$ mg/mL, **a** 46 min 30 s after dropping the suspension, **b** 48 min, **c** 48 min 45 s, **d** 49 min 50 s. Length of the bar is 10 μm

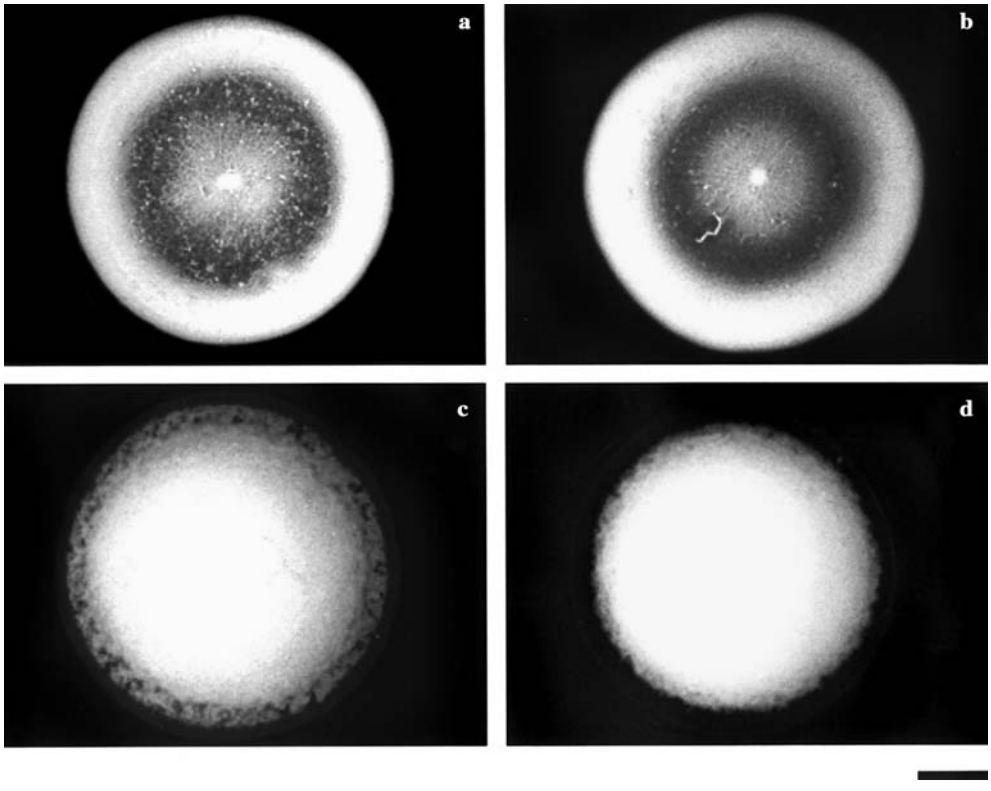

Fig. 8 Patterns formed for 2p7f particles at 25°C. In water, 0.05 mL, $w = 4.6$ mg/mL, **a** NaCl = 0 M, **b** 1×10^{-5} M, **c** 1×10^{-4} M, **d** 1×10^{-3} M. Length of the bar is 2.0 mm

Table 1 The ratio (r) of the long axis against short axis of the outside pattern as a function of the inclined angle (α)

Particles	r					
	$\alpha = 0°$	1.9°	5.2°	8°	11°	19°
Bentonite[a]	1.00	1.01	1.05	–	1.11	1.92
Colloidal silica[b]	1.00	–	1.26	1.86	–	–

[a]In water, $w = 4.6$ mL and 0.05 mL[b]103 nm in diameter, in water, 73.2 mg/mL and 0.1 mL

files shown in Fig. 6a support the existence of the broad ring patterns and do not support existence of the round hills in the center except the suspension of the highest particle concentration. However, the flat and thick regions were observed clearly for the bentonite particles. It should be recalled that the central region of the film of the spherical particles were always extremely thin [1, 2, 10].

The areas (S) covered with the particles in the dried film were 9.7, 19.0, 58, 59, 54, and 60 mm^2 at particle concentrations (w) of 4.6×10^{-4}, 0.046, 0.092, 0.46, 0.92, and 4.6 mg/mL, respectively. S kept very small when w is smaller than 0.05 mg/mL, but increased sharply with further increasing particle concentration. This dependency corresponds that the most particles move to the broad ring regions and dried up but part of the particles distribute whole the film area including the central area. The main reason for this observation will be the fact that the plate-like particles are difficult to move in the translational mode compared with spheres, which move easily by the rotational diffusion on a substrate.

Pattern formation processes in the course of drying

Typical examples of the pattern formation processes of the bentonite suspension are shown in Fig. 7. From Fig. 7a to d the pictures show 46 min 30 s, 48 min, 48 min 45 s and 49 min 50 s after setting the suspensions. The drying frontier moves from right to left with time in the figures. The border between the liquid and solid regions is the frontier zone of drying. Soon after setting the suspensions, vague wrinkle patterns appeared. It is clear that the patterns, which are composed of the accumulated particles, had already formed in the suspension phase, though they were not so fine and clear. As time elapsed, the dry frontier moved to the left side and the vague patterns formed in the liquid phase became clearer and finer in the course of drying. These observations suggest strongly that the patterns grow and are already fixed in the suspension phase. Clearly, the drying patterns kept the same structures basically as those formed in the liquid phase.

Salt concentration dependency

Figure 8 shows the patterns formed in the presence of NaCl. As is clear from comparison among the four pictures, broad ring patterns in the deionized suspension shifted toward the single round hill pattern by the addition of salt. The thickness of the film for the salt containing suspension is shown clearly in Fig. 6b as a function of the distance from the center, r. Clearly, broad ring disappeared completely when the concentration of NaCl is 0.001 M. The suspension became whitey turbid when the concentration of NaCl is higher than 1×10^{-4} M. Association of the plate-like particles is highly plausible. It should be recalled that the dried patterns of colloidal silica spheres in an aqueous suspension became quite rough in the outer edges when NaCl was added [1, 2]. Substantial decrease in the translational movement of the associated particles is one of the main reasons for the very interesting change in the patterns. The area of the patterns first increased slightly, but turned to decrease as the concentration of NaCl increased, i. e., S-values were 60, 70, 71, and 50 mm^2 at NaCl = 0, 1×10^{-5}, 1×10^{-4} and 1×10^{-3} M, respectively.

Drying dissipative structures on an inclined cover glass

Influence of the inclination of the cover glass upon the patterns was also examined in this work. Location of the pattern center shifted to the lower position as the inclination angle (α) increased, though the pictures showing these features are omitted in this paper. Furthermore, the outside broad ring patterns shifted from circle to the egg-shaped. Table 1 shows the ratio (r) of the long axis against short one for the outside shape as a function of α. For comparison, the r-values for the colloidal silica spheres are also listed in the table. Distortion of the outside patterns of the bentonites was not so significant compared with that of spheres, though the experimental conditions such as particle size, particle concentration and amount of the liquid drop, are not the same to each other. This tendency is consistent with the idea that the translational movement of the anisotropic-shaped particles should be much lower than the spherical particles.

References

1. Okubo T, Okuda S, Kimura H (2002) Colloid Polym Sci 280:454
2. Okubo T, Kimura K, Kimura H (2002) Colloid Polym Sci 280:1001
3. Terada T, Yamamoto R, Watanabe T (1934) Sci Paper Inst Phys Chem Res Jpn 27:173; Proc Imper Acad Tokyo 10:10
4. Terada T, Yamamoto R, Watanabe T (1934) Sci Paper Inst Phys Chem Res Jpn 27:75
5. Terada T, Yamamoto R (1935) Proc Imper Acad Tokyo 11:214
6. Okubo T, Kimura H, Kimura T, Hayakawa F, Shibata T, Kimura K (2004) Colloid Polymer Sci 283:1–9
7. Okubo T, Yamada T, Kimura K, Tsuchida A Colloid Polymer Sci (submitted)
8. Okubo T, Kanayama S, Ogawa H, Hibino M, Kimura K (2004) Colloid Polymer Sci 282:230
9. Okubo T, Kanayama S, Kimura K (2004) Colloid Polymer Sci 282:486
10. Kimura K, Kanayama S, Tsuchida A, Okubo T Colloid Polymer Sci (in press)
11. Matsumoto M (1999) Colloids Surfaces A 148:75
12. Matsumoto M (1996) Biophys Chem 58:173
13. Gong T, Wu DT, Marr WMM (2002) Langmuir 18:10064
14. Rowan DG, Hansen JP (2002) Langmuir 18:2063
15. Okubo T, Onoshima D, Kimura K, Tsuchida A (in preparation)
16. Okubo T, Hibino M, Ogawa H, Kimura K, Tsuchida A (in preparation)
17. Okubo T, Togawa H, Kimura K, Tsuchida A (in preparation)
18. Okubo T, Yamaguchi T, Otake A (in preparation)
19. Ohara PC, Heath JR, Gelbart WM (1997) Angew Chem 109:1120
20. Ohara PC, Heath JR, Gelbart WM (1998) Langmuir 14:3418
21. Gelbart WM, Sear RP, Heath JR, Chang S (1999) Faraday Discuss 112:299
22. Tsuchida A, Nakagawa N, Yoshikura K, Okamoto J, Itoh M, Okubo T (in preparation)